Computers and Concrete, *Vol.15, No.2 (2015) 141-166*
DOI: http://dx.doi.org/10.12989/cac.2015.15.2.141

Effect of tube area on the behavior of concrete filled tubular columns

P.K. Gupta*, V.K. Verma, Ziyad A. Khaudhair and Heaven Singh

Department of Civil Engineering, Indian Institute of Technology Roorkee, Roorkee, India

(*Received December 27, 2012, Revised November 10, 2014, Accepted November 15, 2014*)

Abstract. In the present study, a Finite Element Model has been developed and used to study the effect of diameter to wall thickness ratio (*D*/*t*) of steel tube filled with concrete under axial loading on its behavior and load carrying capacity. The model is verified by comparing its findings with available experimental results. Influence of thickness and area of steel tube on strength, ductility, confinement and failure mode shapes has been studied. Strength enhancement factors, load factor, confinement contribution, percentage of steel and ductility index are defined and introduced for the assessment. A parametric study by varying length and thickness of tube has been carried out. Diameter of tube kept constant and equals to 140 mm while thickness has been varied between 1 mm and 6 mm. Equations were developed to find out the ultimate load and confined concrete strength of concrete. Variation of lateral confining pressure along the length of concrete cylinder was obtained and found that it varies along the length. The increase in length of tubes has a minimal effect on strength of tube but it affects the failure mode shapes. The findings indicate that optimum use of materials can be achieved by deciding the thickness of steel tube. A better ductility index can be obtained with the use of higher thickness of tube.

Keywords: concrete filled steel tube (CFST); ductility; confinement; strength; finite element method

1. Introduction

For several decades, finite element method has been dominantly used to analyze various structural engineering problems. Despite of the long history and the success in engineering fields, there have been many unsolved issues in this field. In recent past significant research on concrete filled steel tube (CFST) columns has been conducted to understand their behavior and performance. CFST columns have been increasingly used in multistory buildings and bridges. These composite tubular columns have better structural performance as compared to the R.C.C. and steel columns. In R.C.C. columns, reinforcing bars only confine the concrete core and concrete cover remains unconfined, which spalls off during occurrence of an earthquake. On the other hand in CFST columns the outer steel tube confines the whole concrete core uniformly throughout the length.

*Corresponding author, Professor, E-mail: pkgupfce@iitr.ernet.in

http://www.techno-press.org/?journal=cac&subpage=8 ISSN: 1598-8198 (Print), 1598-818X (Online)

Schneider (1998) tested fourteen specimens having circular, square and rectangular shapes of CFST columns. Out of which only three were of circular shape to investigate the effect of steel tube shape and wall thickness on ultimate strength of concrete column. He reported that for small dimensional CFST columns, smaller diameter to wall thickness ratio (D/t) provides a significant increase in yield load. He also concluded that the specimens having smaller D/t value exhibited more favorable post-yield behavior. Shams and Saadeghvaziri (1999) performed a parametric study using three dimensional finite element model (FEM) to identify the effect of D/t ratio and concrete uniaxial compressive stress on the behavior of CFST columns under axial loading. They found that as D/t value increases the yield stress of steel tube decreases. The decrease in yield stress of steel tube compared to normal yield stress is more significant in columns with higher D/t value and could be as low as 85 percent of the normal yield stress. They proposed an equation which gives relationship between maximum compressive stress in concrete and D/t for both circular and square columns. (Huang *et al*. 2002) tested three circular CFST column specimens having D/t value 40, 70 and 150. They studied the effect of D/t value on the behavior of circular and square columns. They showed that the circular CFST columns having D/t value nearly 40 closely approaches an elastic-perfectly plastic behavior, while columns having D/t value 70 and 150 exhibit strain softening behavior. (Hsuan *et al*. 2003) carried out a nonlinear finite element analysis (FEA) of concrete filled tubular (CFT) columns with circular section, square section and square section stiffened by reinforcing ties to study and analyze the behavior of CFT. They reported that for circular tubes having smaller values of D/t (say $D/t<40$) provides a greater confinement. They proposed an empirical relationship on the basis of FEA, between confining pressure and D/t values for the two ranges of D/t values. The two ranges of D/t values were 21.7 to 47 and 47 to 150. On the basis of these equations, it is clear that as D/t increases, the confining pressure decreases. (Liu *et al*. 2009) carried out experiments on circular tube confined reinforced-concrete (CTRC) columns under cyclic and monotonic axial compression. They developed a relationship between longitudinal stress of the steel and D/t value. (Ellobody *et al*. 2006) carried out parametric study using FEA for specimens having D/t values ranging from 15 to 70. They found that enhancement of column strength was more for specimens having D/t values lower than 55, as compared to the columns having D/t values between 55 and 70.

They (Gupta *et al*. 2004) tested eighty one specimens of CFST columns to investigate the effect of length to diameter (L/D) ratio and diameter to thickness (D/t) ratio of a steel tube on the load carrying capacity of concrete filled tubular columns. The study reported that for smaller D/t values, steel tube provides good confinement effect to the concrete. It was also reported that the load carrying capacity of the steel tube per unit volume decreases as the D/t value increases and hence it was suggested to fix a correct D/t value in order to make optimum usage of the materials. This was also found that for higher value of L/D, specimens which deformed in Euler buckling, the confinement was of lower magnitude. Liang and Sam (2009) carried out parametric study to investigate the effect of D/t value, concrete compressive strength and yield strength of steel on strength and ductility of columns. They reported reduction in axial ductility performance of CFST columns with increase in the D/t value. They also found that circular CFST columns with D/t values ranging from 60 to 100 exhibit strain softening behavior. El-Heweity (2012) conducted a parametric study using FEA to investigate the influence of diameter of concrete filled tubular column and yield stress of steel. The diameters of tubes were 100 mm, 140 mm and 200 mm and yield strength of these steel tubes were 240 MPa, 360 MPa and 520 MPa. He reported that failure

axial strain for smaller diameter specimen was higher as compared to larger diameter specimen. The values of the strains were 0.046 for columns having larger diameter and 0.032 for small diameter columns.

(Abed *et al*. 2013) carried out parametric study with the help of experiments and FEA for the specimens having *D*/*t* values 54, 32 and 20. The compressive strength of concrete was taken 44 MPa and 60 MPa. They reported that the *D*/*t* value is the prime factor which is having more effects on compressive strength of CFST as compared to other factors.

From the literature review it can be concluded that many researchers have studied the effect of *D*/*t* value on load carrying mechanism and behavior of CFST columns having circular cross-section. The results related to the effect of *D*/*t* values were not prime concern of these researchers. Therefore in this paper a systematic computational study using FEA has been conducted. In past two decades FEM has been grown and reached to the state of maturity and FEA results can be used to predict the behavior with good degree of accuracy.

The aim of the paper is three fold: Firstly to develop a FEA model that can predict the behavior of CFST circular columns. Secondly, to analyze the results of the parametric study such as the variation of confinement and ductility with change in *D*/*t* values. Thirdly, to predict the relationship between *D*/*t* values and various parameters like ultimate load, confinement parameter. Finally to predict the best proportion of material between steel and concrete to obtain the optimum use for required behavior of CFST columns.

2. Computer modelling

2.1 Finite element model

A three dimensional Finite element model was developed using ANSYS software to simulate the concrete filled circular steel tube (CFST) under axial compression. To model the concrete core, a three dimensional eight node solid element SOLID 65 was used. To model the steel tube, eight node solid element SOLID 45 was used. Mesh size was chosen from 6 mm to 10 mm for both steel tube and concrete core. Two rigid plates were modeled to simulate rigid cross heads of machine. Load was applied to the column through the top loading plate. In the compression test, direct contact exists between the end plates and end surface of the column; therefore a contact available in ANSYS was used to simulate the interaction between rigid plate and column end surface. The contact was defined as a surface to surface contact.

To activate the confinement of concrete core in finite element model, a contact surface pair comprised of the inner surface of the steel tube and the outer surface of concrete core was adopted. Flexible behavior in the normal direction was assumed with no penetration allowed between the surfaces. A friction factor of 0.2 was obtained and then adopted to achieve a quick convergence and to obtain an accurate result. In finite element model, the lower rigid plate contacting the bottom of column was fixed in all six directions by reference node. The upper rigid plate at the top of the column was modeled fixed in five directions and only allowed movement in column axis at reference node. The load was applied as static uniform displacement at upper rigid plate through the reference node at the center of rigid plate. Fig. 1 shows a typical finite element model adopted for modeling of CFST column.

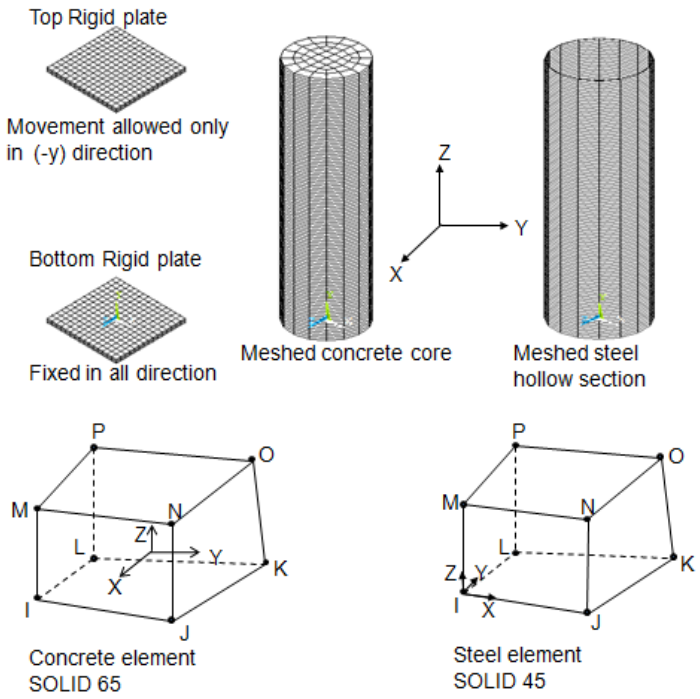

Fig. 1 Typical finite element model for CFST column

2.2. Material model of steel

The material behavior of the steel tube is similar to the reinforcing bars and thus it can be simulated by an elastic-perfectly plastic model. The Poisson's ratio and elastic modulus of steel are taken 0.3 and 200GPa. When steel tube subjected to several stresses, a Von-mises criterion F is used to define the elastic limit, which is written as

$$F = \sqrt{3J_2} = \frac{1}{\sqrt{2}}\sqrt{(\sigma_1-\sigma_2)^2+(\sigma_2-\sigma_3)^2+(\sigma_3-\sigma_1)^2} = \sigma_y$$

where J_2 = Second stress invariant of the stress deviator tensor.

σ_1, σ_2, and σ_3 are the principal stresses.

2.3 Material model of concrete

The response of concrete is modeled by an elastic-plastic theory with associated flow and kinematic hardening rule. The concrete in CFST column is usually subjected to tri-axial compression stresses, the failure of concrete is dominated by compression failure. The Poisson's ratio of concrete material is taken as 0.2

2.3.1 Stress-Strain model for concrete confined by circular steel tube

Fig. 2 shows the uniaxial stress-strain curve for unconfined and confined concrete. The maximum stress of concrete f_{cc} confined by circular steel tube and corresponding strain ε_{cc} have been proposed by (Mander *et al*. 1988).The equations are given as

$$f_{cc} = f_{ck} + k_1 f_l \tag{1}$$

$$\varepsilon_{cc} = \varepsilon_{ck}\left(1 + k_2 \frac{f_l}{f_{ck}}\right) \tag{2}$$

where f_{ck} = Unconfined compressive cylinder strength of concrete;

k_1, k_2 are constant, generally taken as 4.1 and 20.5, (Richart *et al*. 1928).

The value of ε_{ck} for confined concrete may be taken as 0.003 as per ACI (1999)

f_l = Lateral confining stress induced due to confinement provided by steel tube and depends upon D/t and f_y value of tube. They approximate values of f_l can be calculated from the empirical equations given by Hu *et al*. (2009). They proposed two equations to cover the D/t ranges between 21.7 to 150.The equations for the values are given as

$$\frac{f_l}{f_y} = 0.043646 - 0.000832\,(D/t) \qquad \text{for } 21.7 \le D/t \le 47 \tag{3(a)}$$

$$\frac{f_l}{f_y} = 0.006241 - 0.0000357\,(D/t) \qquad \text{for } 47 \le \ D/t \le 150 \tag{3(b)}$$

where D = outer diameter of steel tube;

t = wall thickness of tube; f_y = yield strength of steel tube.

The first part of stress-strain curve shown in Fig. 2 defines the linear property of confined concrete and the proportional limit stress can be assumed to be $0.5f_{cc}$ as given by (Hu *et al*. 2009). The initial Young's Modulus of the confined concrete as per ACI 1999 is given by $E_{cc} = 4700\sqrt{f_{cc}}$ MPa. The Poisson's ratio may be taken as 0.2.

The second part of the stress-strain curve is the nonlinear portion, starts from the proportional limit stress $0.5f_{cc}$, ends at the confined strength f_{cc}. This part was proposed by Saenz (1964), and is given as

$$f = \frac{E_{cc}\varepsilon}{1 + (R + R_E - 2)\left(\frac{\varepsilon}{\varepsilon_{cc}}\right) - (2R - 1)\left(\frac{\varepsilon}{\varepsilon_{cc}}\right)^2 + R\left(\frac{\varepsilon}{\varepsilon_{cc}}\right)^3} \tag{4}$$

where

$$R_E = \frac{E_{cc}\varepsilon_{cc}}{f_{cc}}, \quad R = \frac{R_E(R_\sigma - 1)}{(R_\varepsilon - 1)^2} - \frac{1}{R_\varepsilon}, \tag{5}$$

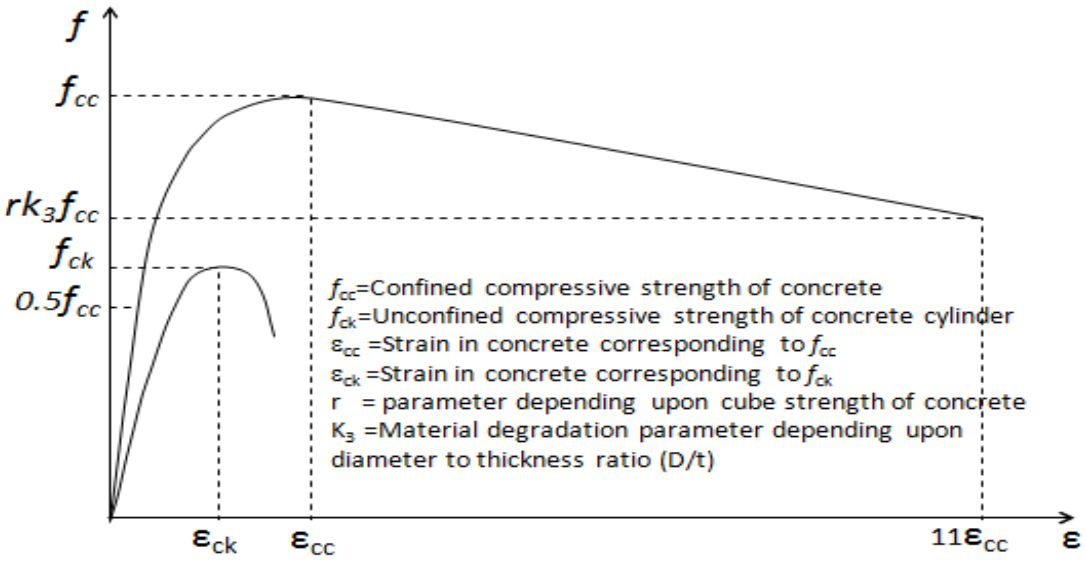

Fig. 2 Stress-strain curves for unconfined concrete and concrete confined by circular steel tube

The values of R_σ and $R_\varepsilon = 4$ as per (Husan *et al*. 2003)

The third part of the curve starts from f_{cc} and ends at $f_u = rk_3 f_{cc}$ with the corresponding strain $\varepsilon_u = 11\varepsilon_{cc}$ (5). The reduction factor k_3 depends upon (D/t) values of tube and having the following values. (Husan *et al*. 2003) proposed the value of k3, and is given as

$$\text{where} \quad k_3 = 1 \quad \text{for } 21.7 \le D/t \le 40 \tag{6}$$

$$k_3 = 0.0000339(D/t)^2 - 0.0100085(D/t) + 1.3491 \tag{7}$$

For $40 \le (D/t \le 150$

The value of r was suggested by (Ellobody *et al*. 2006) and it can be taken as r = 1.0 for concrete with cube strength of 30MPa and 0.5 for concrete with cube strength of 100MPa, respectively. Linear interpolation may be used for concrete with cube strength between 30 and 100 MPa.

3. Parametric study

A parametric study is conducted by modeling of thirty three specimens of concrete filled steel tubes (CFST) of length of 602 mm, 840 mm and 1120 mm with external diameter of 140 mm for each tube with the varying thickness of steel tubes from 1 mm to 6 mm shown in Table 1. The effect of D/t ratio, L/D ratio and percentage area of steel tube is studied. The variation of load

carrying capacity, ductility and confinement of CFST columns are studied. The compressive strength of unconfined concrete, f_c and yield stress of steel tube were kept constant. Values of f_c

Table 1 Geometrical and material properties of CFST column specimens

Specimen	Dimensions (mm)			Ratios		Material Properties (MPa)	
	Outer diameter (D)	Thickness (t)	Length	D/t	L/D	f_c	f_y
A1	140	1.0	602	140	4.3	28.18	285.0
A2	140	1.5	602	93.33	4.3	28.18	285.0
A3	140	2.0	602	70.0	4.3	28.18	285.0
A4	140	2.5	602	56.0	4.3	28.18	285.0
A5	140	3.0	602	46.67	4.3	28.18	285.0
A6	140	3.5	602	40.0	4.3	28.18	285.0
A7	140	4.0	602	35.0	4.3	28.18	285.0
A8	140	4.5	602	31.11	4.3	28.18	285.0
A9	140	5.0	602	28.0	4.3	28.18	285.0
A10	140	5.5	602	25.45	4.3	28.18	285.0
A11	140	6.0	602	23.33	4.3	28.18	285.0
B1	140	1.0	840	140	6.0	28.18	285.0
B2	140	1.5	840	93.33	6.0	28.18	285.0
B3	140	2.0	840	70.0	6.0	28.18	285.0
B4	140	2.5	840	56.0	6.0	28.18	285.0
B5	140	3.0	840	46.67	6.0	28.18	285.0
B6	140	3.5	840	40.0	6.0	28.18	285.0
B7	140	4.0	840	35.0	6.0	28.18	285.0
B8	140	4.5	840	31.11	6.0	28.18	285.0
B9	140	5.0	840	28.0	6.0	28.18	285.0
B10	140	5.5	840	25.45	6.0	28.18	285.0
B11	140	6.0	840	23.33	6.0	28.18	285.0
C1	140	1.0	1120	140	8.0	28.18	285.0
C2	140	1.5	1120	93.33	8.0	28.18	285.0
C3	140	2.0	1120	70.0	8.0	28.18	285.0
C4	140	2.5	1120	56.0	8.0	28.18	285.0
C5	140	3.0	1120	46.67	8.0	28.18	285.0
C6	140	3.5	1120	40.0	8.0	28.18	285.0
C7	140	4.0	1120	35.0	8.0	28.18	285.0
C8	140	4.5	1120	31.11	8.0	28.18	285.0
C9	140	5.0	1120	28.0	8.0	28.18	285.0
C10	140	5.5	1120	25.45	8.0	28.18	285.0
C11	140	6.0	1120	23.33	8.0	28.18	285.0

and f_y were taken equal to 28.18 MPa and 285 MPa respectively. The lateral confining pressure (f_l) and confined strength of concrete is calculated with the help of confining model. Poisson's ratio of concrete and steel were taken as 0.2 and 0.3 respectively to attain the minimum level of confinement. The strength of the specimens and their load-compression variation were obtained from this parametric study.

4. Verification of model

The past experimental data available in literature are used to validate the developed model. To validate the model for different CFST specimens having different geometric proportions were chosen from literature. Table 2 summarizes the geometries and material properties of these specimens. The specimens were chosen in such a way so that wall thickness between 1 mm and 7 mm can be covered. Figs. 3 (a)-(f)) shows the comparison of load-compression curves of three specimens. It is clear from this figure that good agreement presents between predicted and experimental curves. The deflected shape of a representative specimen is also compared and found in good agreement (see Fig. 4)

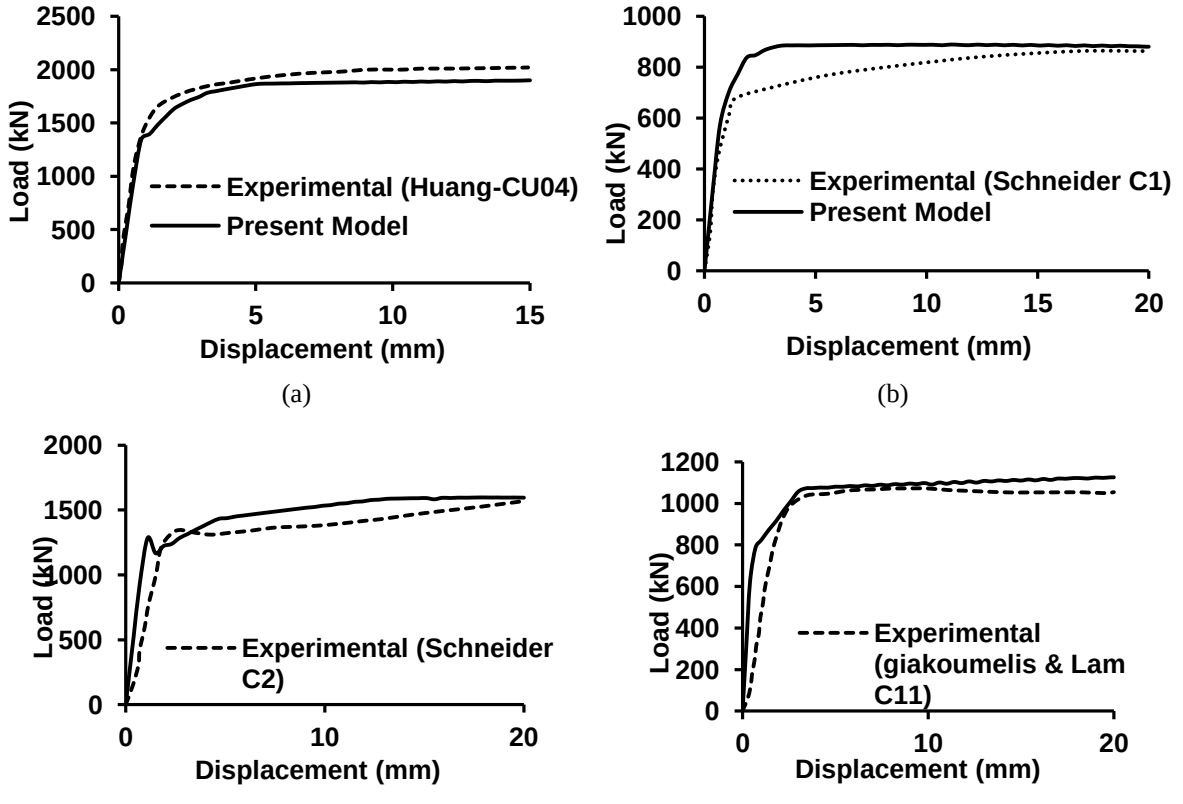

Fig. 3 (a)-(f)) Comparison of Load-displacement variations

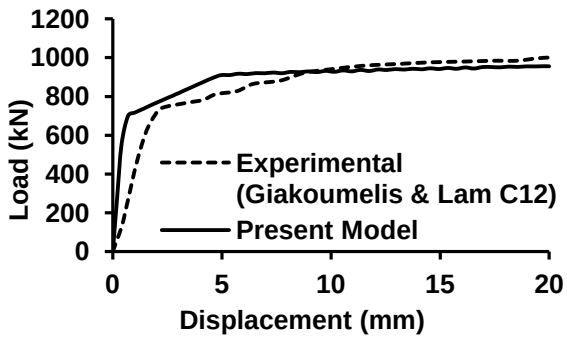

(e)

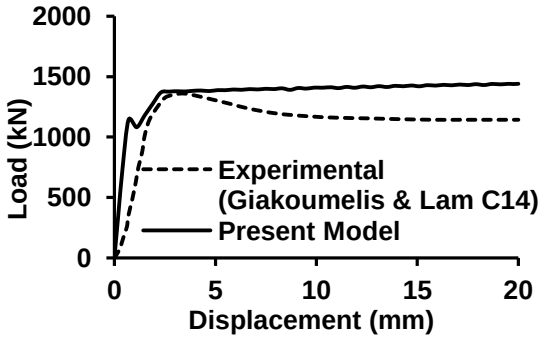

(f)

Fig. 3 (a)-(f)) Continued

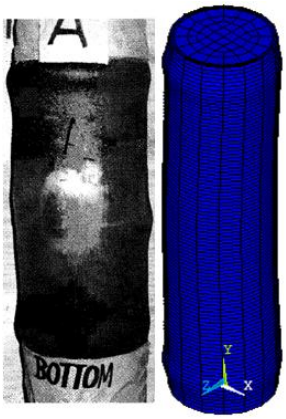

Schneider Present Model

Fig. 4 Comparison of mode of deformation

Table 2 Verification of computational model

Specimen	Reference	Dimensions (mm)			Ratios		Material Properties (MPa)	
		Outer diameter, D	Thickness, t	Length	D/t	L/D	f_c	f_y
C1	Schneider (1998)	140	3.0	602	47.0	4.3	28.18	285.0
C2		141	6.5	602	21.7	4.3	23.8	313.0
CU-040	(Huang *et al*. 2002)	200	5.0	600	40.0	3.0	27.15	265.8
C11	Giakoumelis and Lam (2004)	114	3.75	300	30.5	2.62	25.52	343.0
C12		114	3.85	300	29.7	2.62	46.08	343.0
C13		114	3.84	300	29.8	2.62	79.12	343.0

5. Results and discussions

The developed Finite element model has been used to compress thirty three specimens for the axial displacement up to 20 mm. The obtained load-compression variations are presented in Figs. 5(a)-(c)). For specimens having three wall thickness t = 1 mm, 3 mm and 6 mm with L/D = 4.3, 6.0 and 8.0, the compression process was simulated up to 100 mm of compression to obtain the typical results in greater detail. Figs. 6-8 show the deformed shapes and corresponding load-compression variation of these specimens. It is clear from Figs. 6-8 that the load becomes almost steady after 20 mm deformation of CFST columns. The different results of CFST columns obtained from load-compression curves are presented in Table 3(a), 3(b), 3(c). The effect of D/t for various L/D values on the confinement, strength and ductility are shown in Figs. 9-11. The relationship between confined strength of concrete, unconfined strength of concrete and D/t ratio has been developed in form of an equation. The variation of ultimate load with respect to lateral confining pressure and percentage of steel are shown in Figs. 12 and 13 respectively. Equations have been obtained to find out ultimate load capacity and confined concrete strength. Axial stress distribution at critical sections of CFST columns for 20 mm axial displacement have been shown in Figs. 14(a)-(l)) for different specimens having L/D = 4.3 and thickness from 1mm to 6 mm. It can be seen from the graph that maximum stress is at the Centre of the section in most of the cases and it is approximately equals to the maximum stress of confined concrete calculated and shown in the Table 3(a)-(c)).

Table 3(a) Results showing ultimate load, ductility index, confinement contribution, strength enhancement factor for CFST with L/D ratio equals to 4.3

Sp-eci-men	D/t	E_1 Joule	E_2 Joule	% of steel, p	μ	f_l/f_c	Ultimate load, Pu kN	Load, P kN	ζ	As*f kN	f_{cc} MPa	S_f
A1	140.0	426	4090	2.92	9.60	0.013	568	546	4.03	125	29.62	1.05
A2	93.33	495	5520	4.42	11.15	0.029	660	602	9.63	186	32.16	1.14
A3	70.00	499	5570	5.97	11.16	0.038	739	656	12.65	247	33.87	1.20
A4	56.00	510	5800	7.55	11.37	0.043	800	711	12.51	308	34.37	1.22
A5	46.67	577	6710	9.15	11.63	0.049	888	765	16.08	368	36.87	1.31
A6	40.00	614	7140	10.8	11.63	0.105	982	819	19.90	428	39.88	1.42
A7	35.00	660	7820	12.5	11.85	0.147	1100	873	26.00	487	44.79	1.59
A8	31.11	690	8410	14.2	12.19	0.180	1200	926	29.59	546	48.52	1.72
A9	28.00	728	8980	16.0	12.34	0.206	1300	979	32.79	604	52.44	1.86
A10	25.45	759	9480	17.8	12.49	0.227	1380	1031	33.85	662	54.94	1.95
A11	23.33	792	9940	19.6	12.55	0.245	1450	1083	33.89	720	56.73	2.01

Table 3(b) Results showing ultimate load, ductility index, confinement contribution, strength enhancement factor for CFST with L/D ratio equals to 6.0

Sp-eci-men	D/t	E_1 Joule	E_2 Joule	% of steel, p	μ	f_l/f_c	Ultimate load, P_u kN	Load P	ξ	As*fy kN	f_{cc} MPa	S_f
B1	140.0	525	5350	2.92	10.19	0.013	553	546	1.28	125	28.61	1.02
B2	93.33	592	6490	4.42	10.96	0.029	640	602	6.31	186	30.80	1.09
B3	70.00	635	7350	5.97	11.57	0.038	706	656	7.62	247	31.60	1.12
B4	56.00	669	8020	7.55	11.99	0.043	765	711	7.60	308	31.93	1.13
B5	46.67	727	8740	9.15	12.02	0.049	831	765	8.62	368	32.83	1.17
B6	40.00	804	9860	10.8	12.26	0.105	975	819	19.04	428	39.37	1.40
B7	35.00	880	10810	12.5	12.28	0.147	1100	873	26.00	487	44.79	1.59
B8	31.11	900	11170	14.2	12.41	0.180	1200	926	29.59	546	48.52	1.72
B9	28.00	910	12300	16.0	13.51	0.206	1300	979	32.79	604	52.44	1.86
B10	25.45	920	13000	17.8	14.13	0.227	1370	1031	32.88	662	54.17	1.92
B11	23.33	940	13700	19.6	14.57	0.245	1440	1083	32.96	720	55.95	1.99

Table 3(c) Results showing ultimate load, ductility index, confinement contribution, strength enhancement factor for CFST with L/D ratio equals to 8.0

Sp-eci-men	D/t	E_1 Joule	E_2 Joule	% ste-el, p	μ	f_l/f_c	Ultimate load, P_u kN	Load P	ξ	As*fy kN	f_{cc} MPa	S_f
C1	140.0	610	6890	2.92	11.30	0.013	554	546	1.47	125	28.68	1.02
C2	93.33	660	8610	4.42	13.05	0.029	630	602	4.65	186	30.12	1.07
C3	70.00	740	9810	5.97	13.26	0.038	701	656	6.86	247	31.25	1.11
C4	56.00	730	10760	7.55	14.74	0.043	766	711	7.74	308	32.00	1.14
C5	46.67	790	11720	9.15	14.84	0.049	831	765	8.63	368	32.83	1.17
C6	40.00	879	13310	10.8	15.14	0.105	977	819	19.3	428	39.52	1.40
C7	35.00	950	14600	12.5	15.37	0.147	1090	873	24.9	487	44.06	1.56
C8	31.11	1010	15700	14.2	15.54	0.180	1190	926	28.5	546	47.78	1.70
C9	28.00	1050	16700	16.0	15.90	0.206	1280	979	30.8	604	50.93	1.81
C10	25.45	1090	17600	17.8	16.14	0.227	1360	1031	31.9	662	53.41	1.90
C11	23.33	1140	18800	19.6	16.49	0.245	1430	1083	32.0	720	55.18	1.96

Table 4 Maximum longitudinal and hoop stress in steel tube at different sections of CFST

Thickness of tube, t (mm)	D/t	L/D	Yield stress of steel, f_y (MPa)	Stresses at critical section (MPa)		Stresses at normal section (MPa)	
				Longitudinal	Hoop	Longitudinal	Hoop
1	140	4.3	285	278.548	139.256	277.889	38.082
3	46.67	4.3	285	286.742	40.643	293.364	73.819
6	23.33	4.3	285	284.371	167.273	296.771	103.637

The programme was run for 100 mm displacement to get the better deflected mode shapes. It can be clearly seen from Figs 6-8 that bulging occurs in the CFST tube having thickness of 1 mm. For the tube thickness of 3 mm and 6 mm, local buckling was seen under axial loading. A slight bulging at different location with local buckling throughout the length was seen for the tube having thickness from 3.5 to 6.0 mm for 20 mm displacement.

Fig. 15(a) shows the variation of the confining pressure at different compression stages along the length of the specimens having L/D = 4.3 and t = 6 mm. The confining pressure along the length of the specimen is not constant. The confining pressure is almost zero up to the yield point, which is due to the difference of Poisson's ratio between steel and concrete. As the compression process progresses the confining pressure starts developing and reaches to their maximum value at 100 mm of compression. The confining pressure is highest at the bottom platen-tube and top platen-tube interface. This may be due to the interfacial friction. The confinement starts after the yielding; it is verified from the Fig. 15(b). Fig. 15(b) shows the axial stress distribution in concrete at 1 mm displacement. The values of axial stress at every point are less than the unconfined strength of concrete. Fig. 16 shows the typical steel tube with location of critical and normal sections. The longitudinal and hoop stresses in steel tube were obtained from simulations at critical and normal sections to compare with yield stress of steel as shown in Table 4. The hoop stresses are lower in magnitude at normal sections as compared to the corresponding critical sections. This is due to the bulging of steel tube at critical section.

5.1 Capacity aspects

From Fig. 5, it can be seen that load carrying capacity increases with the increase in thickness of steel tube for all L/D values. There is no significant change obtained in the ultimate load with the varying L/D values. The axial capacity of column increases from 568 kN to 1440 kN with the increase in thickness from 1 mm to 6 mm. This improvement in load carrying capacity is partially due to the increase in confinement of concrete core with increase in thickness of steel tube. Confinement contribution based on load carrying capacity of CFST columns is calculated from ultimate load determined from developed model. A parameter ξ has been chosen to represent the confinement provided by steel tubes. The confinement contribution, ξ in percentage may be obtained as;

$$\xi = \left(\frac{P_u - P}{P}\right) x100$$

where P_u= ultimate load capacity obtained from model

$$P = f_y A_{sc} + f_c A_c$$

where f_y = yield stress of steel,

A_{sc}= cross-sectional area of steel tube

f_c= unconfined compressive strength of concrete

A_c=cross- sectional area concrete core

Fig. 9 shows the effect of D/t ratio on confinement contribution on axial capacity of column for all L/D values. The minimum value of confinement contribution (ξ) is 1.28 % for the tube of 1 mm thickness and maximum value is 33.89 % for the tube of 6.0mm thickness. Fig 12 shows the variation in the load factor (P_u/P) with the change in the ratio of lateral confining pressure to

unconfined strength of concrete (f_l/f_c). Fig 12 shows the variation of P_u/P with percentage of steel (p) used for steel tube in CFST columns. It is clear from Fig. 12 that as the ratio of f_l/f_c increases the ratio of P_u/P also increases. It is also clear that a definite relationship exists between these two parameters. Therefore two equations have been obtained one gives relationship between P_u/P and f_l/f_c and other gives relationship between P_u/P and p.

$$\frac{P_u}{P} = [1.2095\ (\frac{f_l}{f_c}) + 1.0693] \tag{8}$$

$$\frac{P_u}{P} = [0.0191\ p + 1] \tag{9}$$

where P_u= ultimate load capacity

$P = f_y A_{sc} + f_c A_c$

f_l = lateral confining pressure (MPa)

f_c = strength of unconfined concrete (MPa)

$p = (A_s/A_c) \times 100$= percentage of steel

5.2 Strength aspect

Concrete strength increases due to increase in confining pressure for varying thickness of steel tubes (1 mm to 6.0 mm). An enhancement factor defined as (S_f) has been used to see the improvement in the strength of concrete. The term S_f represents the ratio of the strength of confined concrete (f_{cc}) to the strength of unconfined concrete (f_c). The term f_{cc} is determined using the following equation

$$f_{cc} = \frac{(P_u - A_s f_y)}{A_c} \text{ and } S_f = \frac{f_{cc}}{f_c}$$

Fig. 10 shows the improvement in concrete strength with the increase in thickness of tube. However slight difference in the value of S_f is noticeable for CFST with different L/D ratios. It is also clear from Table 3(a), 3(b) and 3(c) that the value of S_f varies from 1.02 to 2.01 for CFST columns having L/D values from 4.3 to -8.0. It may be stated from findings that the strength increases with increase in confinement due to the increase in thickness of tube. Equations have been developed to predict f_{cc} from D/t for two ranges of D/t values. These equations are;

$$f_{cc} = f_c\,[-0.0316\,(D/t) + 2.7316] \qquad \text{for } 23.33 \le D/t \le 47 \tag{10}$$

$$f_{cc} = f_c\,[-0.0021(D/t) + 1.3383] \qquad \text{for } 47 < D/t \le 140 \tag{11}$$

5.3 Ductility aspect

The effect of change of thickness of steel tube on ductility performance is studied. Since there is no clear definition of ductility of concrete, a new parameter (i.e., ductility index) is adopted (10). It is expressed in terms of stored energy during displacement. The ductility index $\mu = E_2/E_1$, where E_2 is the area under load-strain curve up to strain at 80% of ultimate load after peak load for strain softening behavior of material, that strain comes out to be 1.38%) . Similarly for strain hardening the area under the curve is taken up to strain of 1.38 % (E_1 is the area underneath the curve up to elastic limit as shown in Fig. 17. Ductility index may give the idea about the energy absorption by post elastic deformation. Load-displacement curves for energy calculation are given from Fig 5. The value of two calculated energy parameters E_1 and E_2 are listed in Table 3(a), 3(b) and 3(c). The results indicate that the value of ductility index varies from 9.6-16.5 for all types of CFST columns. While varying the value of L/D ratio from 4.3 to 8.0, there is no significant difference in ductility index.

5.4 Ductility aspect

The proposed equations are verified using the experimental results given in the literature. It was found that results obtained from the equations are in good agreement with experimental results. Table 5(a) presents the comparison of obtained results using developed equations between ultimate load and ratio of confining pressure and compressive strength of concrete. Table 5(b) presents the comparison of obtained results using developed equations between ultimate load and percentage of steel. Figs. 18(a) and 18(b) show the curves between calculated and experimental values of ultimate load. The curves show the linear behavior between the experimental and calculated values.

Table 5 (a) Verifications of proposed equation to predict ultimate load capacity with confinement (Equation no.8)

Reference	CFST	Dimensions (mm)			Material Properties (MPa)		Lateral confining pressure f_l MPa	Ulti-mate Load, P_{exp} kN	Ulti-mate Load, Pu, kN from equa-tion 8
		Outer dia. (D)	Thick-ness (t)	Length (L)	f_c	f_y			
(Husan *et al.* 2003)	CU-022	140	6.5	602	23.80	313.0	8.00	1666.0	1673.0
	CU-040	200	5.0	840	27.15	265.8	2.85	2016.9	1895.0
	CU-047	140	3.0	602	28.18	285.0	1.30	893.00	860.00
	CU-070	280	4.0	840	31.15	272.6	1.00	3025.2	3058.0
	CU-100	300	3.0	900	27.23	232.0	0.97	2810.0	2795.0
	CU-150	300	2.0	840	27.23	341.7	0.30	2607.6	2721.0

Table 5 (b) Verifications of proposed equation to predict ultimate load capacity with different percentage of steel. (Equation no.9)

Reference	CFST	% of steel p	Dimensions (mm)				Material Properties (MPa)		Ulti-mate Load, P_{exp} kN	mate Load, P_u, kN from equa-
			Outer dia. (D)	Thick-ness (t)	D/t	L/D	f_c	f_y		
Schneider (1998)	C1	9.15	140	3.00	47.00	4.30	28.18	285.0	881.00	899.00
(Huang *et al*. 2006)	CU040	10.8	200	5.00	40.00	3.00	27.15	265.8	2013.0	1901.0
	CU070	5.97	280	4.00	70.00	3.00	31.15	272.6	3025.0	3058.0
	CU150	2.72	300	2.00	150.0	3.00	27.23	341.7	2608.0	2639.0
O'shea and Bridge (2000)	S10CS50A	1.84	190	0.86	221.0	3.47	41.00	210.7	1350.0	1293.0
	S12CS50A	2.42	190	1.13	168.1	3.50	41.00	185.7	1377.0	1317.0
	S16CS50B	3.28	190	1.52	125.0	3.50	48.30	306.1	1695.0	1700.0
	S30CS50B	7.20	165	2.82	58.51	3.52	48.30	363.3	1662.0	1690.0
(Sakino *et al*. 2004)	CC4-A-2	8.45	149	2.96	50.40	-	25.40	308.0	941.00	960.00
	CC6-A-2	16.7	122	4.54	26.90	-	25.40	576.0	1509.0	1584.0
(Oliveira *et al*. 2009)	C-30-3D	12.85	114.3	3.35	34.11	3.00	32.70	287.3	737.00	785.00

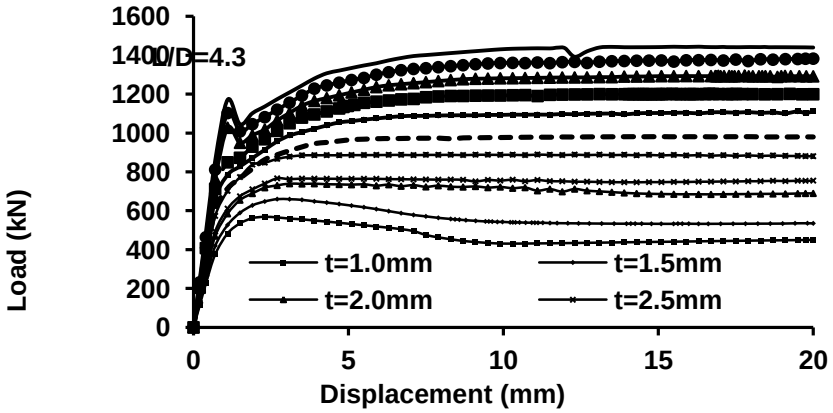

Fig. 5 (a) Load-displacement curve for CFST with different thickness of tubes with L/D=4.3 and outer diameter =140 mm

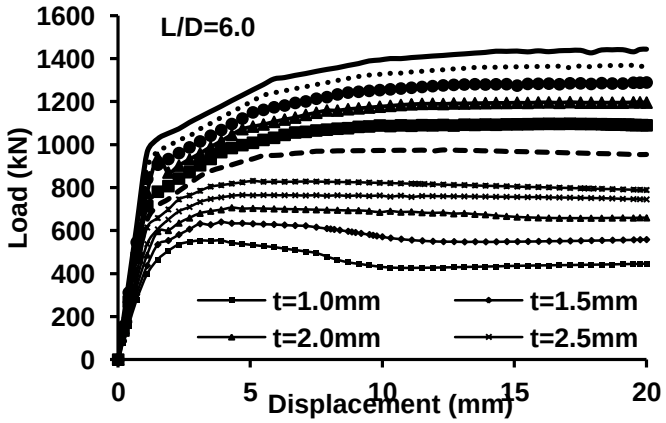

Fig. 5 (b) Load-displacement curve for CFST with different thickness of tube with *L*/*D*=6.0 and outer diameter = 140 mm

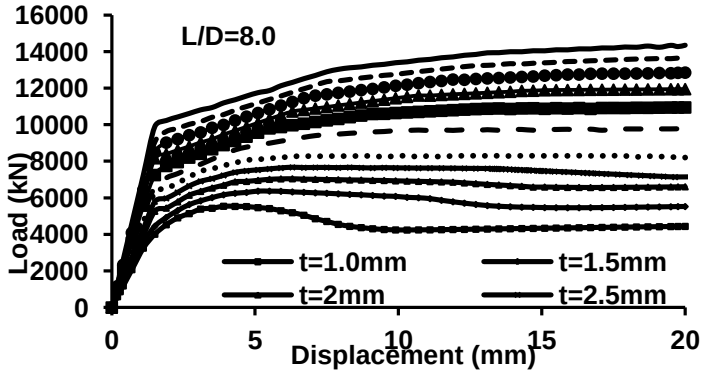

Fig. 5 (c) Load-displacement curve for CFST with different thickness of tube with *L*/*D*=8.0 and outer diameter = 140 mm

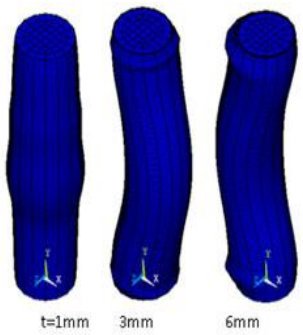

Fig. 6(a) Mode of deformation of CFST at 100 mm deformation for t = 1 mm, 3 mm and 6 mm with L/D =4.3

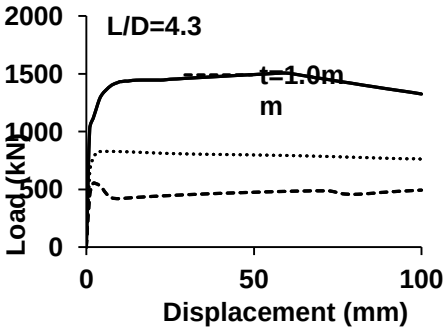

Fig. 6(b) Load-displacement curve for 100mm displacement for CFST with thickness of tube (t)= 1 mm, 3 mm and 6 mm with L/D = 4.3

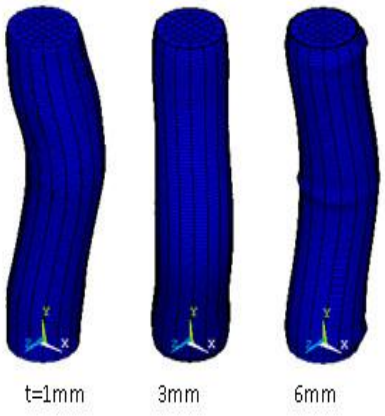

Fig. 7(a) Mode of deformation of CFST at 100 mm deformation for t = 1 mm, 3 mm and 6 mm with L/D =6.0

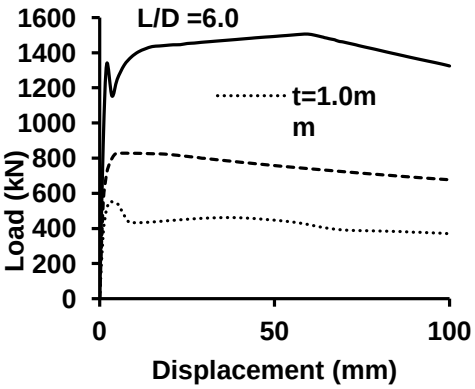

Fig. 7(b) Load-displacement curve for 100mm displacement for CFST with thickness of tube (t)= 1 mm, 3 mm and 6 mm with L/D =6.0

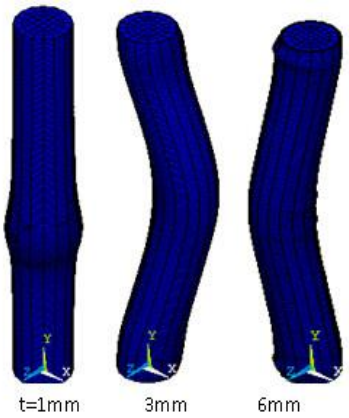

Fig. 8(a) Mode of deformation of CFST at 100 mm deformation for t = 1 mm, 3 mm and 6 mm with L/D = 8.0

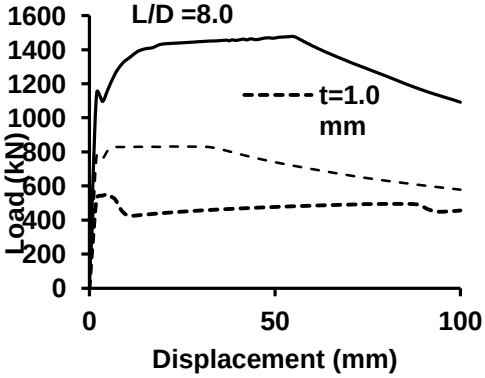

Fig. 8(b) Load-displacement curve for 100 mm displacement for CFST with thickness of tube (t) = 1 mm, 3 mm and 6 mm with L/D = 8.0

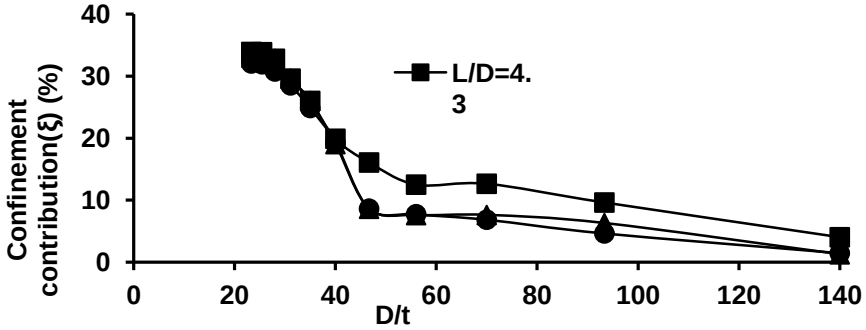

Fig. 9 Effect of D/t ratio on confinement contribution of CFST column

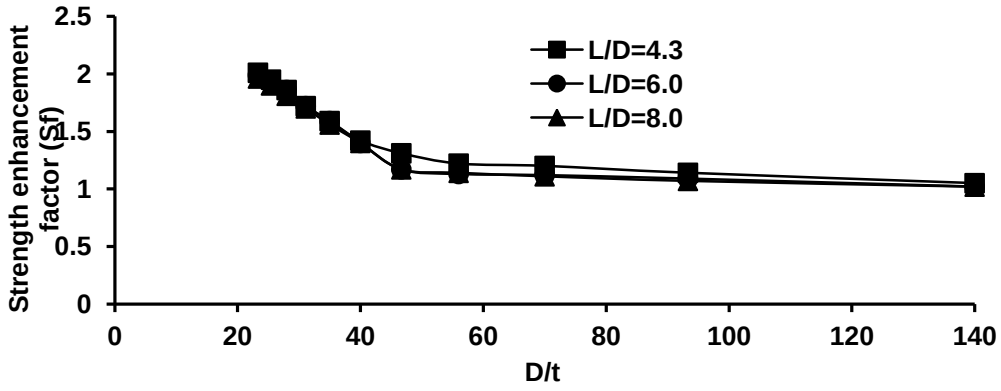

Fig. 10 Effect of *D*/*t* ratio on strength enhancement of CFST column

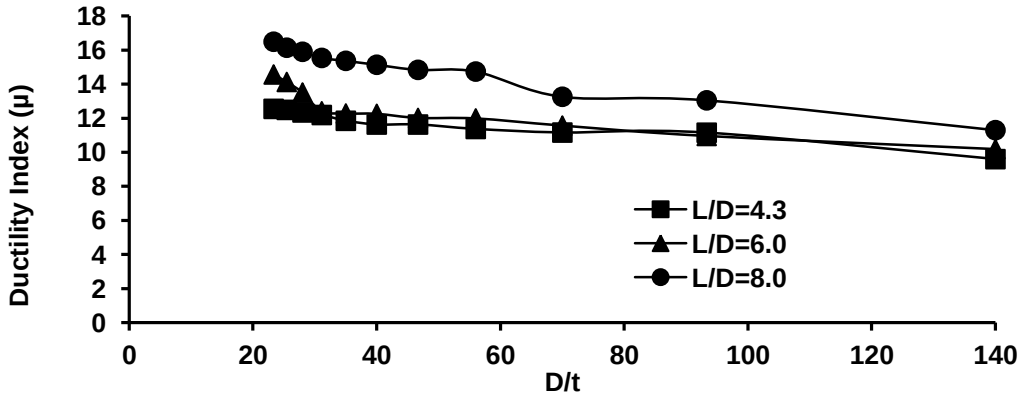

Fig. 11 Effect of *D*/*t* ratio on ductility index of CFST column

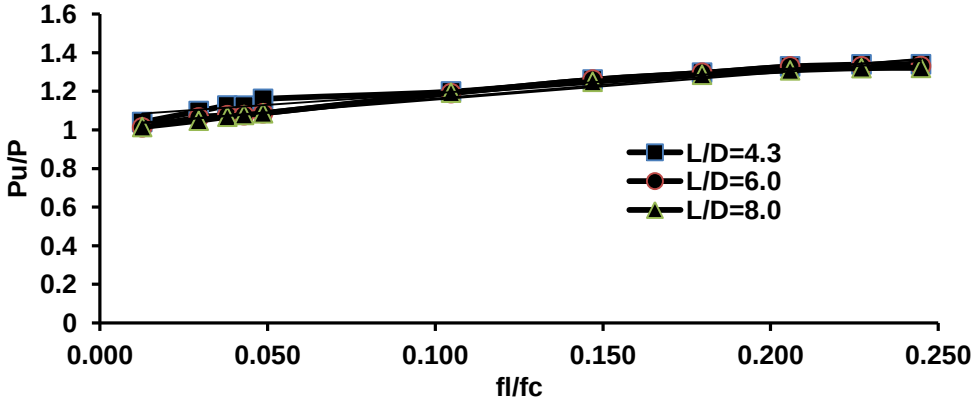

Fig. 12 Effect of f_l/f_c on load factor of CFST column

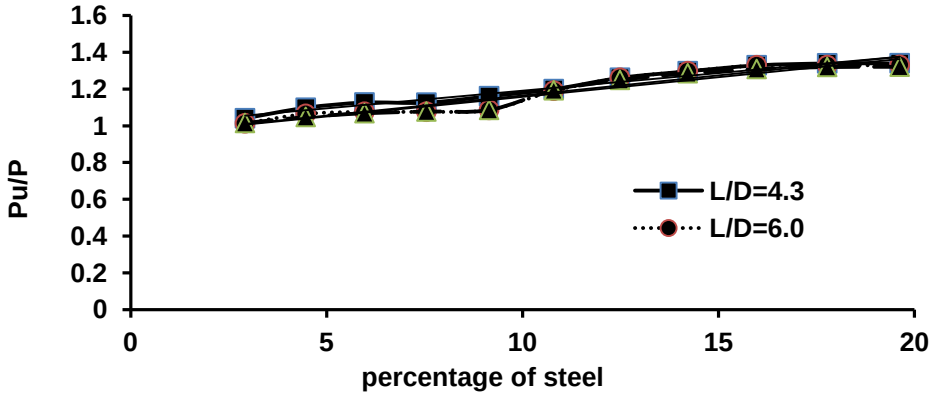

Fig. 13 Effect of percentage of steel on load factor of CFST column

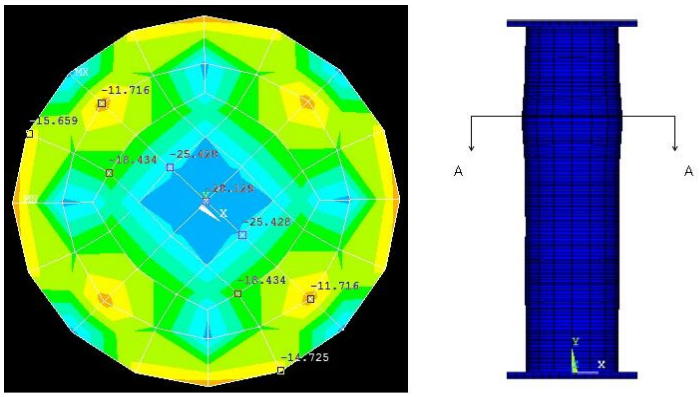

Fig. 4(a) Axial stress (MPa) distribution in concrete at section A-A for 20 mm compression of CFST with L/D = 4.3 and t = 1 mm

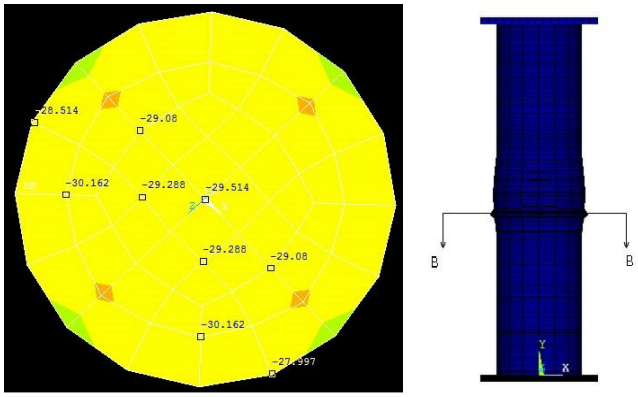

Fig. 14(b) Axial stress (MPa) distribution in concrete at section B-B for 20 mm compression of CFST with L/D = 4.3 and t = 1.5 mm

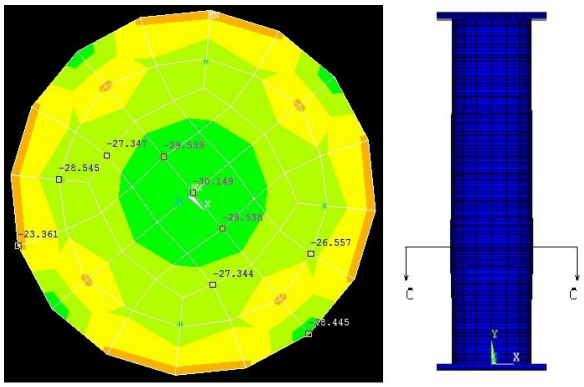

Fig. 14(c) Axial stress (MPa) distribution in concrete at section B-B for 20 mm compression of CFST with L/D = 4.3 and t = 1.5 mm

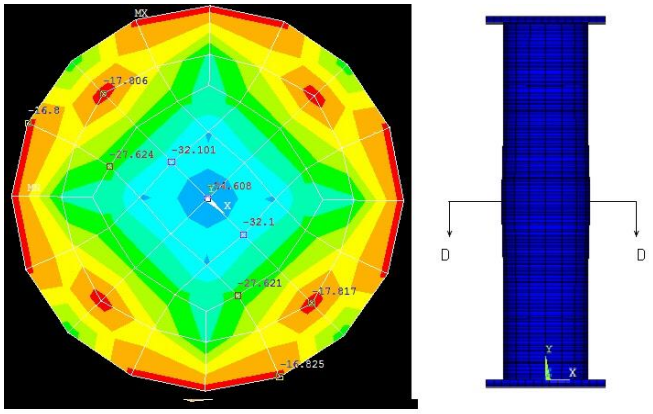

Fig. 14(d) Axial stress (MPa) distribution in concrete at section B-B for 20 mm compression of CFST with L/D = 4.3 and t = 1.5 mm

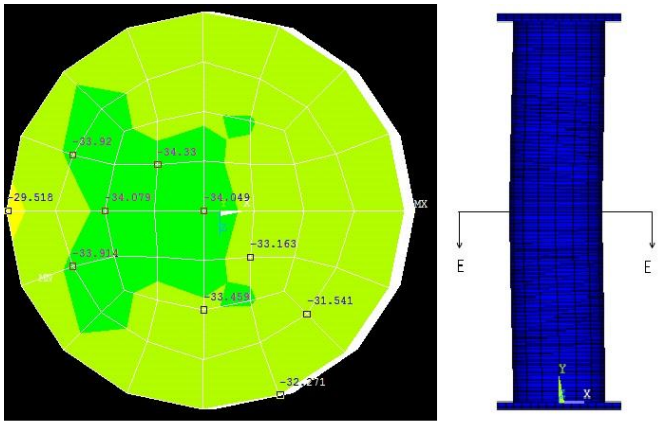

Fig.14(e) Axial stress (MPa) distribution in concrete at section B-B for 20 mm compression of CFST with L/D = 4.3 and t = 1.5 mm

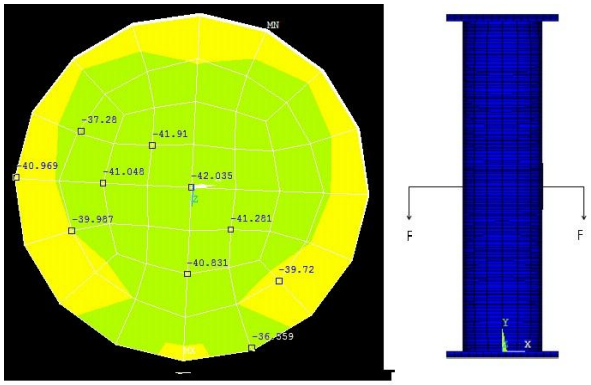

Fig. 14(f) Axial stress (MPa) distribution in concrete at section F-F for 20 mm compression of CFST with L/D = 4.3 and t = 3.5 mm

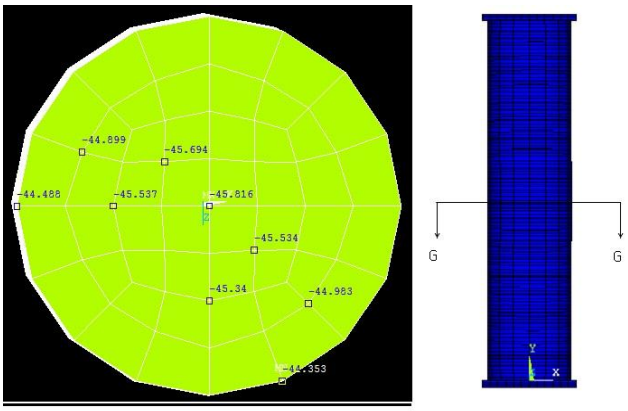

Fig. 14(g) Axial stress (MPa) distribution in concrete at section F-F for 20 mm compression of CFST with L/D = 4.3 and t = 3.5 mm

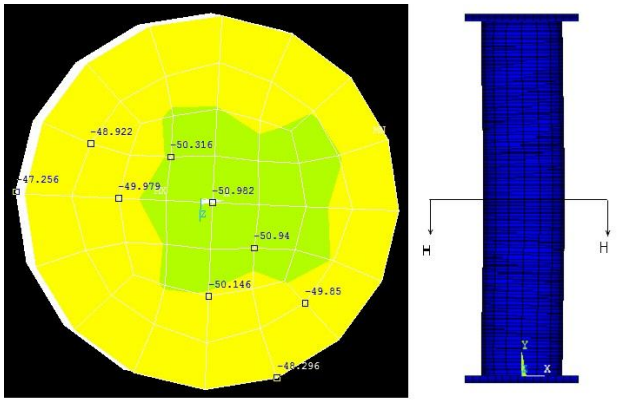

Fig. 14(h) Axial stress (MPa) distribution in concrete at section F-F for 20 mm compression of CFST with L/D = 4.3 and t = 3.5 mm

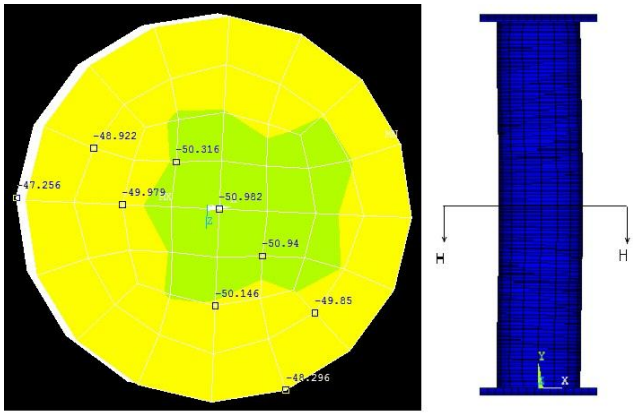

Fig. 14(i) Axial stress (MPa) distribution in concrete at section F-F for 20 mm compression of CFST with L/D = 4.3 and t = 3.5 mm

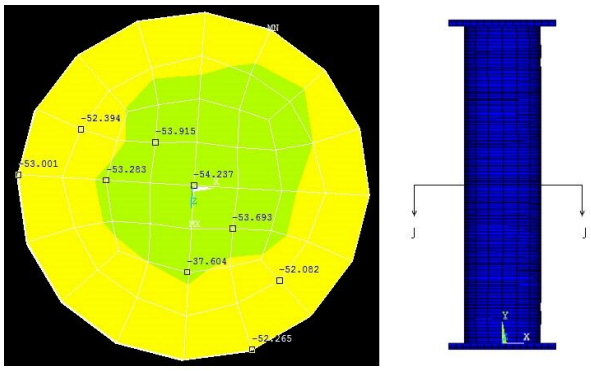

Fig. 14(j) Axial stress (MPa) distribution in concrete at section F-F for 20 mm compression of CFST with L/D = 4.3 and t = 3.5 mm

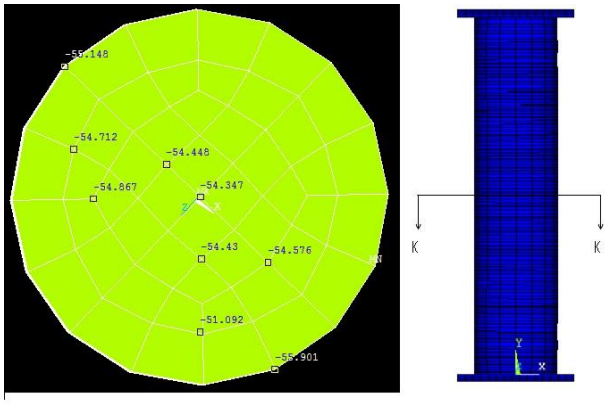

Fig. 14(k) Axial stress (MPa) distribution in concrete at section F-F for 20 mm compression of CFST with L/D = 4.3 and t = 3.5 mm

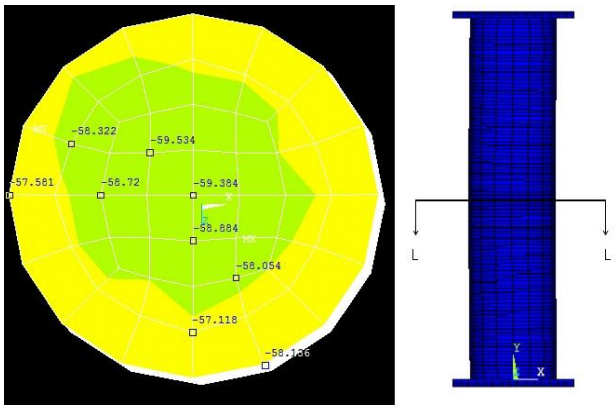

Fig. 14(l) Axial stress (MPa) distribution in concrete at section F-F for 20mm compression of CFST with L/D = 4.3 and t = 3.5 mm

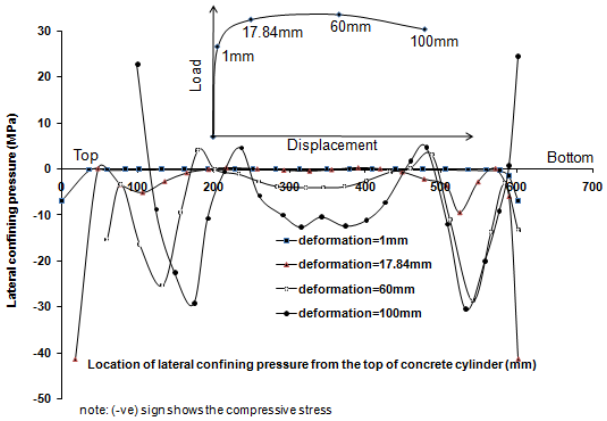

Fig. 15 (a) Typical Variation of lateral confining pressure along the length of concrete cylinder at different deformation for CFST having thickness of steel tube = 6 mm, L = 602 mm and L/D = 4.3

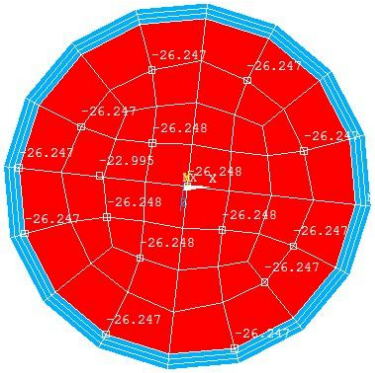

Fig. 15 (b) Typical Variation of axial stress (MPa) distribution in concrete for 1mm compression at critical section for CFST having thickness of steel tube (t) =6 mm and L/D = 4.3

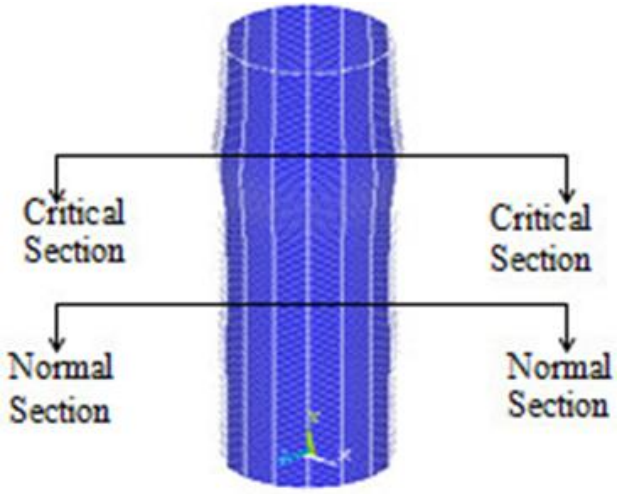

Fig. 15 (b) Typical Variation of axial stress (MPa) distribution in concrete for 1 mm compression a tcritical section for CFST having thickness of steel tube (t) =6 mm and L/D=4.3

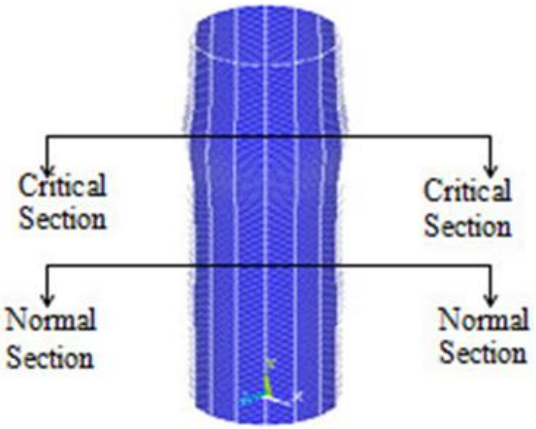

Fig. 16 Typical steel tube showing critical section and normal section for the calculation of hoop and longitudinal stresses

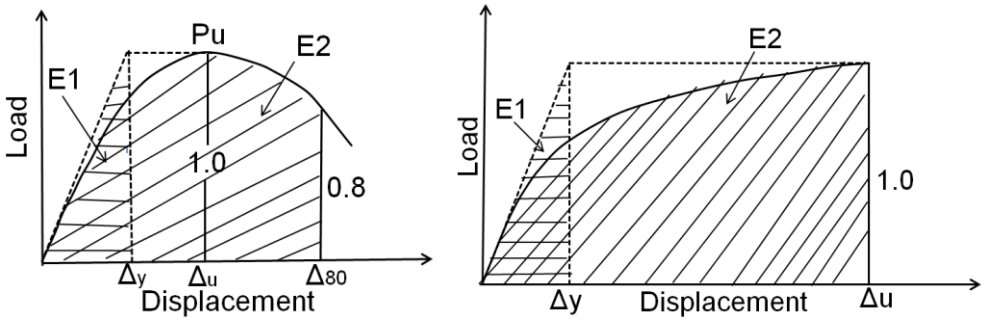

Fig. 17 Definition of ductility

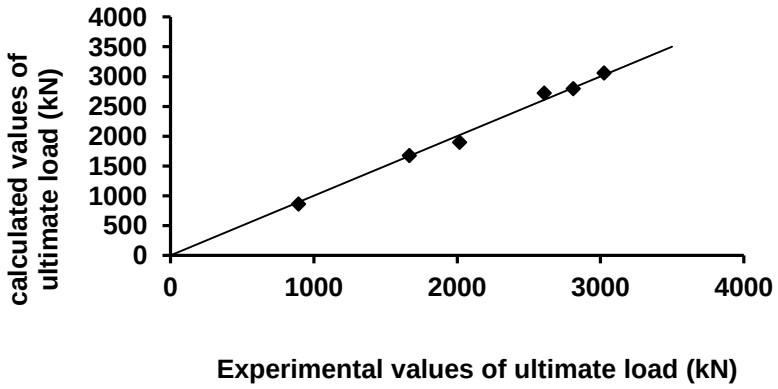

Fig. 18(a) Verification of equation no. 8 to predict ultimate load capacity

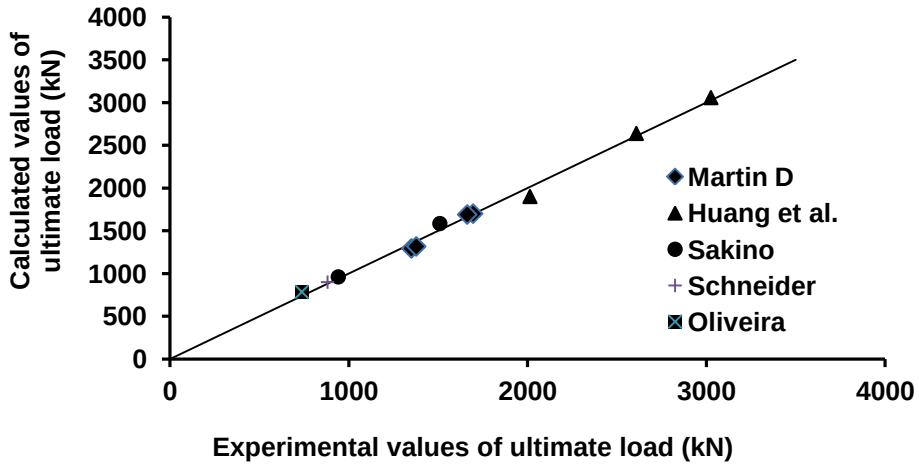

Fig. 18(b) Verification of equation no. 9 to predict ultimate load capacity

6. Conclusion

Following points can be concluded on the basis of results obtain from present Finite element analysis of concrete filled steel tubular (CFST) columns.

- A better ductility index can be obtained with the use of about 9.15 % of steel.
- Enhancement of concrete strength is shown from 2.0 to 101% due to confinement obtained with steel varying from 2.92 to 19.6 percent.
- The confinement contribution increases with increase in percentage of steel. It is as low as 1.28 % for steel percentage of 2.92 and as high as 34 % for steel percentage of 19.6.
- Simplified equations have been proposed to calculate the ultimate load carrying capacity and confined concrete strength of CFST columns. The adequacies of equations have been validated with experimental results available in literature.

- The lateral confining pressures have been found out at different stage of deformation of the CFST column along the length of concrete core. It may be concluded that the lateral confining pressure (f_l) does not remain constant during compression process.

References

ACI (1999), "Building code requirements for structural concrete and commentary", *Am. Concrete Inst*., ACI 318-99, Detroit (USA).

Ellobody, E., Young, B. and Lam, D. (2006), "Behaviour of normal and high strength concrete filled compact steel tube circular stub columns", *J. Constr. Steel Res*., **62**, 706-715.

Farid, A., Mohammad, A., Suliman, A. (2013), "Experimental and numerical investigation of the compressive behavior of concrete filled steel tubes (CFSTs)", *J. Constr. Steel Res*.**, 80**, 429-439.

Giakoumelis, G. and Lam, D. (2004), "Axial capacity of circular concrete filled tube columns", *J J. Constr. Steel Res*., **60**, 1049-1068.

Gupta, P.K., Sarda, S.M. and Kumar, M.S. (2007), "Experimental and computational study of concrete filled steel tubular columns under axial loads", *J. Constr. Steel Res*.**, 63**, 182-193.

Hu, H.T., Huang, C.S., Wu, M.H. and Wu, Y.M. (2009), "Nonlinear analysis of axially loaded concrete filled tube columns with confinement effect", *J. Struct. Eng*., **129(**10), 1322-1231.

Huang, C.S., Yeh, Y.K., Liu, G.Y., Hu, H.T., Tsai, K.C., Weng, Y.T., Wang, S.H. and Wu, M.H. (2002), "Axial load behavior of stiffened concrete filled steel columns", *J. Struct. Eng*., **128(**9), 1222-1230.

Hsuan-Teh,, Hu, Huang, Chiung-Shiann, Ming-Hsien, and Yih-Min, Wu (2003), "Nonlinear analysis of axially loaded concrete-filled tube columns with confinement effect", *J. Struct. Eng*., **129(**10), 1322-1329.

Liang, Q.Q. and Sam, F. (2009), "Nonlinear analysis of circular concrete filled steel tubular short columns under axial loading", *J. Constr. Steel Res*., **65**, 2186-2196.

Liu, J., Sumei, Z., Xiaodong, Z. and Lanhui, G. (2009), "Behaviour and strength of circular tube confined reinforced concrete columns", *J. Constr. Steel Res*., **65**, 1447-1458.

Mahamed Mahmoud El- Heweity (2012), "On the performance of circular concrete filled high strength steel columns under axial loading", *Alexandria Eng. J*., 1-12.

Mander, J.B., Priestley, M.J.N. and Park, R. (1988), "Theoritical stress-strain model for confined concrete*"*, *J. Struct. Eng*., **114(**8), 1804-1830.

O'shea, Martin, D. and Bridge Russell, Q. (2000), "Design of circular thin walled concrete filled steel tubes", *J. Struct. Eng*., **126**(11), 1295-1303.

Oliveira, W.L.A., Nardin, S.D., Debs, A.L.H.C.E. and Debs, M.K.E. (2009), "Influence of concrete strength and length/diameter on the axial capacity of CFT columns", *J. Constr. Steel Res*., **65**, 2103-2110.

Richart, F.E., Brandzaeg, A. and Brown, R.L. (1928), "A study of the failure of concrete under combined compressive stresses", Bull185, Champaign (IL, USA); University of Illinios Engineering Experimental station.

Saenz, L.P. (1964), "Discussion of 'Equation for the stress-strain curve of concrete' by P.Desayi, and S. Krishnan", *J. Am. Concrete Inst*., **61**, 1229-1264.

Sakino, K., Nakahara, H., Morino, S. and Nishiyama, I. (2004), "Behavior of centrally loaded concrete filled steel tube short columns", *J. Struct. Eng*., **130(**2), 180-188.

Schneider, S.P. (1998), "Axially loaded concrete filled steel tubes", *J. Struct. Eng*., **124(**10), 1125-1138.

Shams, M. and Saadeghvaziri, M.A. (1999), "Nonlinear response of concrete filled steel tubular columns under axial loading", *ACI Struct. J*., **96(**6), 1009-1018.